Circularly polarized surface coil with a single port

Y. Soutome[1], H. Habara[1], and Y. Bito[1]
[1]Central Research Laboratory, Hitachi Ltd., Kokubunji, Tokyo, Japan

Introduction

A quadrature (QD) surface coil, as shown in Fig. 1(a), can improve the signal-to-noise ratio (SNR) by a factor of $\sqrt{2}$ compared with that of a single coil [1,2]. This is because the two orthogonal coils that comprise the QD surface coil can receive a circularly polarized (CP) B_1 field. However, implementation of the QD surface coil is more difficult than that of a single coil because the QD surface coil consists of two coils, baluns, ports, and a QD hybrid circuit. Previously, two surface coils mutually coupled to a single feeding loop have been demonstrated to successfully detect the CP B_1 field [3]. We have designed a CP surface coil with a single port without a mutually coupled loop and have investigated its RF characteristics. The design concept of this coil was based on a CP birdcage coil with a single port [4]. We have also fabricated a CP surface coil and compared its phantom images with those of the QD surface coil.

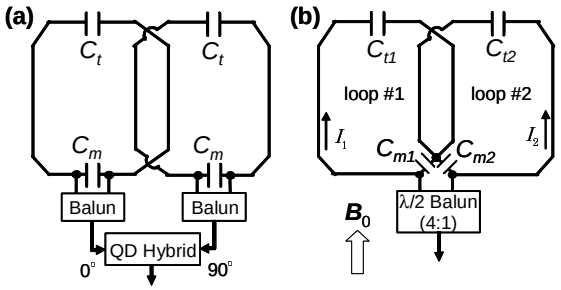

Fig. 1 QD surface coil (a) and CP surface coil with a single port (b)

Method

Coil Design: A schematic diagram of the designed coil is shown in Fig. 1(b). The coil was constructed with two series connected loop-coils each having dimensions of 140 × 200 mm with an overlap of 26 mm. The coil was placed on the outer side of the 290-mm diameter cylinder. The coil was tuned to 127.8 MHz (3.0 T) and matched to 200 Ω. A λ/2 balun converted the impedance of the coil to 50 Ω. The values of the capacitors (C_{t1}, C_{t2}, C_{m1}, C_{m2}) were designed to provide a phase difference of 90° between the currents of loop #1 (I_1) and loop #2 (I_2). The C_{t1}, C_{t2}, C_{m1}, and C_{m2} were 3.26, 3.93, 88, and 23.4 pF, respectively. *Simulations:* We numerically simulated characteristics of the coils using our own program, which was based on the electromagnetic method of moments and impedance analysis [5]. This program can be used to calculate the impedance and sensitivity of the coils with the load. The load was 250 mm in diameter and 70 mm in length. The conductivity and relative permittivity of the load were 0.8 S/m and 78, respectively. Coil sensitivity was defined by the strength of the clockwise, circularly polarized B_1 field (B_1^+) generated by the coil when a signal of 1 W was applied to the coil. *Measurement:* We used an SE sequence on a 3T MR scanner (Varian INOVA) to acquire phantom images. Transmission of the B_1 field was by means of a body coil. The sequence parameters were TR/TE = 1000/30 ms, BW = 53.8 kHz, slice thickness = 5 mm, FOV = 300 × 300 mm, matrix size = 256 × 256, and NEX = 1. A cylindrical phantom (252 mm in diameter and 70 mm in length) was placed near the coil, as shown in Fig. 2. The phantom was filled with a 10-mM $NiCl_2$ and 0.4-wt% NaCl solution. The SNRs of the images were calculated from the ratio of the signal mean value to the standard deviation of noise.

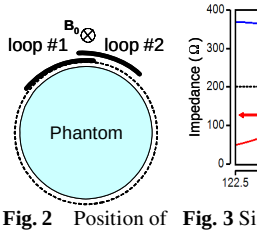

Fig. 2 Position of coil and phantom

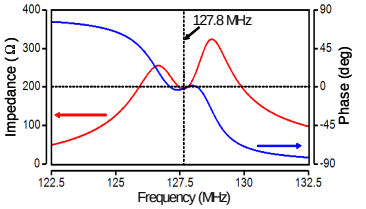

Fig. 3 Simulation results of the impedance characteristics of CP surface coil

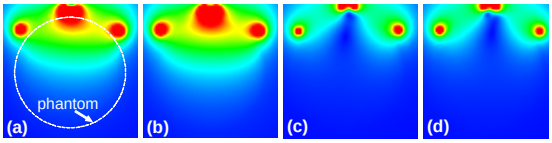

Fig. 4 Simulated results of sensitivity map (300 × 300 mm) for CP(a), QD(b), anti-CP(c), and anti-QD(d) surface coils

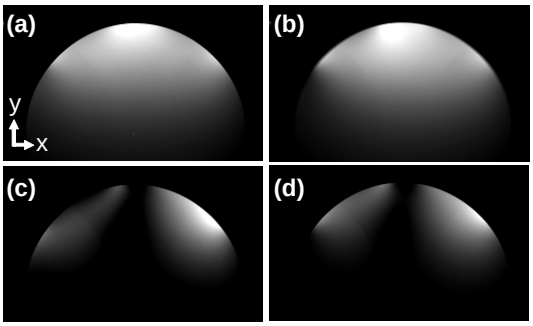

Fig. 5 Phantom images of CP (a), QD (b), anti-CP (c), and anti-QD (d) surface coils

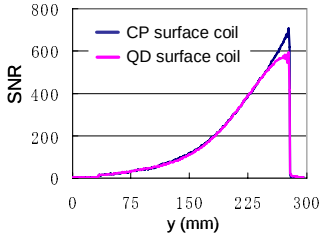

Fig. 6 SNR profiles of phantom images of CP and QD surface coils

Results and Discussion

Figure 3 shows the simulated impedance characteristics of the CP surface coil with the load. Two impedance peaks were observed near the magnetic resonance frequency of 3.0T (127.8 MHz). However, the designed coil showed its maximum sensitivity at 127.8 MHz between the two peaks. Figure 4(a) and 4(b) show sensitivity maps at 127.8 MHz for CP and QD surface coils, respectively. Both maps were very similar. Figure 4(c) and 4(d) show sensitivity maps for the CP surface coil that was rotated 180° (anti-CP) and an anti-QD surface coil, respectively. Both maps were also very similar, and the sensitivity of these coils was observed to be very low in the upper regions of the phantom. This is because the rotation direction of the detected B_1 field was reversed. Figure 5 shows phantom images of CP, QD, anti-CP, and anti-QD surface coils. These phantom images were similar to the sensitivity maps shown in Fig. 4. The phantom images of the CP and anti-CP surface coils were very similar to those of the QD and anti-QD surface coils, respectively. Figure 6 shows SNR profiles of the images shown in Fig. 5(a) and 5(b). These SNR profiles were measured along the y direction through the center of the phantom image. The SNR at the center of the phantom image was 109. The SNR profile of the CP surface coil was identical to that of the QD surface coil except in the region that was close to the conductor of the coil. These results indicate that the CP surface coil can receive the circularly polarized B_1 field as in the case of the QD surface coil.

Conclusion

We have designed and fabricated a circularly polarized surface coil with a single port. Using RF simulations and phantom experiments, we demonstrated that our coil can receive a circularly polarized B_1 field without having a QD hybrid like that of the QD surface coil.

References [1] C.-N. Chen, et al., J. Magn. Reson. 54, 324-327 (1983) [2] G. H. Glover, et al., J. Magn. Reson. 64, 255-270 (1985)
[3] S. M. Wright, SMRM 7th Annual Meeting, *Work in Progress*, 137 (1988)
[4] Y. Soutome, et. al., ISMRM 15th Annual Meeting, 1057 (2007) [5] H. Ochi, et al., SMRM 11th Annual Meeting, 4021 (1992)